Research Article

For reprint orders, please contact: reprints@futuremedicine.com

Nanomedicine

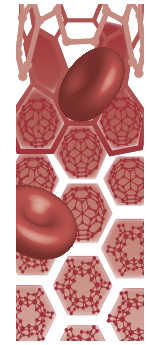

PEGylated graphene oxide for tumor-targeted delivery of paclitaxel

Aim: The graphene oxide (GO) sheet has been considered one of the most promising carbon derivatives in the field of material science for the past few years and has shown excellent tumor-targeting ability, biocompatibility and low toxicity. We have endeavored to conjugate paclitaxel (PTX) to GO molecule and investigate its anticancer efficacy. **Materials & Methods**: We conjugated the anticancer drug PTX to aminated PEG chains on GO sheets through covalent bonds to get GO-PEG-PTX complexes. The tissue distribution and anticancer efficacy of GO-PEG-PTX were then investigated using a B16 melanoma cancer-bearing C57 mice model. **Results**: The GO-PEG-PTX complexes exhibited excellent water solubility and biocompatibility. Compared with the traditional formulation of PTX (Taxol®), GO-PEG-PTX has shown prolonged blood circulation time as well as high tumor-targeting and -suppressing efficacy. **Conclusion**: PEGylated graphene oxide is an excellent nanocarrier for paclitaxel for cancer targeting.

Keywords: cancer therapy • drug delivery • graphene oxide • paclitaxel

Hongyang Xu[1], Minmin Fan[1], Abdelbary MA Elhissi[2], Zhirong Zhang[1], Ka-Wai Wan[3], Waqar Ahmed[3], David A Phoenix[4] & Xun Sun*,[1]

[1]Key Laboratory of Drug Targeting & Drug Delivery Systems, Ministry of Education, West China School of Pharmacy, Sichuan University, Chengdu 610041, PR China

[2]College of Pharmacy, Qatar University, Doha, Qatar

[3]Institute of Nanotechnology & Bioengineering, School of Pharmacy & Biomedical Sciences, University of Central Lancashire, Preston, UK

[4]Office of the Vice Chancellor, London South Bank University, 103 Borough Road, London, SE1 0AA, UK

*Author for correspondence:
Tel.: +86 28 85502307
Fax: +86 28 85501615
xunsun22@gmail.com

Graphene has a hexagonal packed structure formed by a 2D single layer of carbon atoms [1,2]. Owing to its unique properties, graphene and its derivatives have attracted tremendous attention in the fields of electronics, energy, materials and biomedical applications [3–6]. Although the naked GO did not exhibit any obvious *in vitro* toxicity nor *in vivo* inflammation at low concentration [7,8], proper surface functionalization is essential to design graphene-based nanocarrier systems with high solubility in the physiological fluids and acceptable biocompatibility for biomedical application in physiological environments. Various types of hydrophilic polymers have been utilized to functionalize graphene oxide (GO) using covalent or noncovalent bonding [9]. Functionalized GO has been used for drug and gene delivery [9–21], as well as in biosensor platforms, photothermal therapy and in tumor and cell imaging [11,22–32]. Numerous types of polymers and molecules are possible to use for modifying the surfaces of GO via hydrogen bonding or π–π interactions [9,33]. Many aromatic chemotherapy drug molecules can be conjugated onto the surface of GO through physical adsorption, resulting in changing GO from poorly soluble sheets to water-soluble conjugates [10–12,34]. Dai *et al.* first loaded a water insoluble anticancer analog of camptothecin (CPT) onto GO surface through noncovalent conjugation via π–π interaction. The GO loaded with SN38 exhibited acceptable biocompatibility and excellent solubility both in aqueous and physiological solutions [10]. Several research groups have studied targeted delivery of doxorubicin (DOX) and CPT attached to surface modified GO, which exhibited superior anticancer efficacy [12,16,19,21,34]. Despite its lower optical properties, the 2D shape and ultra-small sizes of GO may offer many advantages comparing with other carbon-based nanomaterials such as single-walled nanotubes (SWNTs). For example, the *in vitro* toxicity of graphene towards human cells appears to be lower than that of SWNTs. Moreover, the photothermal

Future Medicine part of fsg

anticancer efficacy of graphene is superior to that of SWNT because of the better dispersion and smaller size of graphene nanoparticles.

Liu *et al.* have first reported that GO modified by coating its surfaces with PEG (GO-PEG) can become highly aqueous soluble and stable in physiological fluids such as serum [10]. These findings can make the *in vivo* intravenous application of GO feasible. Moreover, GO-PEG has shown significant passive tumor-targeting ability, which might be ascribed to the enhanced permeability and retention effect of tumor tissue [35]. The long-term *in vivo* biodistribution and toxicity investigations have demonstrated that GO-PEG exhibited no obvious tissue toxicity, and no organ damage or inflammation symptoms [35,36], which revealed the superior characteristics of GO-PEG compared with uncoated GO [37]. According to Liu *et al.*, following intravenous injection of GO-PEG, the formulation has accumulated in the reticuloendothelial systems (RES) such as liver and spleen and were gradually cleared out via renal excretion and biliary pathway into feces over time [36,38,39].

Paclitaxel (PTX) is a widely used chemotherapeutic drug that promotes tubulin polymerization and formation of extraordinarily dysfunctional and stable microtubules, disrupting the normal tubule dynamics [40]. However, its poor aqueous solubility is a serious limitation that prevents proper formulation and clinical application of the drug [41]. In order to overcome low aqueous solubility of PTX, formulations based on Cremophor EL (e.g., Taxol®) have been prepared and used via slow intravenous infusion following dilution with NaCl (0.9%) or dextrose (5%) solutions. However, the solvent system mainly Cremophor EL in Taxol causes serious toxicological effects [42] such as neurotoxicity and nephrotoxicity, which may significantly reduce the overall therapeutic benefit of PTX. Therefore, Cremophor EL-free delivery systems of PTX have been proposed, including those based on polymeric nanoparticles, polymeric micelles, liposomes and many prodrug formulations [43–47]. Owing to the advantages and unique performance of GO as a targeting system, formulations of PTX loaded onto modified GO are worth exploring.

Unlike DOX and CPT, PTX has no extend π-structure larger than one aromatic ring [48]; hence, it is difficult to load PTX onto GO by physical adsorption. Even though some paper has reported the successful noncovalent conjugation of PTX and GO [49], the loading capacity may be optimized using other methods. Thus, we have investigated the possibility of loading PTX onto GO-PEG through covalent conjugation, aiming to improve the drug physiological solubility and enhance the formulation compatibility and cancer targeting ability. In this work we used GO-PEG as a drug carrier to load PTX via an ester bond, which is cleavable after *in vivo* injection. The covalent conjugation has been reported to be successful at attaching PTX to SWNTs and α,β-Poly(*N*-2-hydroxyethyl)-DL-aspartamide (PHEA) [41,50]. The influence of GO-PEG-PTX conjugation on drug solubility in water and mouse serum was investigated. Moreover, further *in vivo* investigations were carried out to evaluate the anticancer efficacy of GO-PEG-PTX, the blood circulation time, drug bioavailability, tissue distribution and tumor-uptake rate. The *in vivo* biodistribution of GO-PEG-PTX was also investigated and compared with that of Taxol. To the best of our knowledge, this is the first study that demonstrated the feasibility of using PEGylated GO as nanocarriers for PTX and investigated the anticancer activity of the resultant complex compared with Taxol.

Experimental section

Materials

GO was purchased from Tianjin Plannano Technology Co., Ltd. Chloroacetic acid was purchased from Fuchen Chemical Reagents Factory (Tianjin, China). N-(3-dimethylamino propyl-N′-ethylcar-bodiimide) hydrochloride (EDC-HCl), N-hydroxysuc-cinimide (NHS), Succinic anhydride and pyridine were purchased from Kelong Chemical Reagents Factory (Chengdu, China). PTX and docetaxel were purchased from Hao-xuan Biological Technology Co., Ltd (Xi'an, China). Aminated PEG (NH_2-PEG-NH_2, Mw = 4000) was purchased from Kaizheng Biological Technology Co., Ltd, (Beijing, China). Cholesterol esterase was purchased from Shifeng Biological Technology CO., Ltd (Shanghai, China). DMEM cell culture medium was bought from Thermo Fisher Scientific (MA, USA). fetal bovine serum was supplied by Fumeng Gene Co., Ltd (Shanghai, China). 3-(4,5-dimethylthiazol-2-yl)-2,5-diphenyltetrazolium bromide (MTT) was supplied by Sigma (CA, USA). BCA protein assay reagent kit was purchased from Thermo Fisher Scientific.

Cell lines & animals

A549 and B16 melanoma cancer cell lines were purchased from the Type Culture Collection of the Chinese Academy of Sciences (Shanghai, China). C57 mouse and Wistar rats were provided by Chengdu Dashuo Biotechnology Co., Ltd. All procedures with animals were conducted in accordance with institutional animal care and use guidelines.

Carboxylation of GO

To carboxylate GO sheet, GO (10 mg) was added to water and sonicated to form an aqueous suspension. NaOH (0.12 g/ml) and chloroacetic acid (0.5 g) were then added, and the resultant mixture was sonicated using probe sonicator for 3 h to form carboxyl group on

the surface of GO. GO-COOH suspension was neutralized and purified by centrifugation at 10,000 rpm. The supernatant was discarded and the residue was washed with water twice.

Modification of GO with aminated PEG

Carboxylated GO was diluted by water (10 ml) and then bath sonicated with amino-terminated PEG4000 (100 mg) for 30 min, followed by addition of N-(3-dimethylaminopropyl-N′-ethylcarbodiiminde) hydrochloride (EDC-HCl) to reach a concentration of 40 mmol/l. Then the mixture was allowed to react overnight. The final reactants were dialyzed in dialysis bags (molecular weight cutoff = 100,000) for 4 days to obtain the PEGylated GO.

Fourier transform infrared (IR) absorbance spectrum, atomic force microscopy and UV-vis spectrum were used to identify whether the carboxylation and PEGylation were successful.

Synthesis of 2′-O-succinyl-PTX derivative

PTX (200 mg) and succinic anhydride (0.3 g) were added to 5 ml of anhydrous pyridine. The solution was stirred for 24 h at room temperature. The progress of reaction was detected by thin-layer chromatography ($CH_3OH/CHCl_2$ 1:20 v/v). After that, 6 ml of water was added and stirred for 1 h at 60°C. The solvent (pyridine and water) was then evaporated under vacuum at 55°C using a rotary evaporator (BUCHI Rotavapor R-3). The resultant modified PTX was retrieved via extraction using ethyl acetate as solvent. Purification of the desired compounds was carried out by column chromatography on silica gel (the elution phase was $CH_3OH/CHCl_2$ 1:50 v/v). ^{1}H-NMR ($CDCl_3$) and LC-MS were employed to confirm the chemical structures.

Conjugation between GO-PEG & 2′-O-succinyl-PTX

To synthesize GO-PEG-PTX, 2′-O-succinyl-PTX (20 mg) and GO-PEG aqueous solution (~0.4 mg/ml) were dissolved in DMSO-water component solvent (1:1 v/v) followed by addition of EDC-HCl (50 mg) and NHS (50 mg). The resultant solution was stirred at 25°C for 6 h, followed by 2 days of dialysis in DMSO and another 2 days in water. HPLC was used for identification of the conjugation of GO-PEG-PTX.

HPLC analysis

HPLC assay methods were established for the detection of PTX concentration in cellular uptake, pharmacokinetics and biodistribution studies. Analysis was performed using Shimadzu instruments (Chiyoda-Ku, Kyoto, Japan) consisting of a 50 µl injector loop, a CTO-10A column thermostat, two LC-10AT pumps and an Diamonsil C18 reverse phase column. The column effluent was monitored at 227 nm with a flow rate of 1 ml/min at 35°C. The mobile phase was composed of acetonitrile and water (45: 55 v/v). The total run time for each sample was 15 min.

In vitro release behavior of PTX from GO-PEG-PTX

GO-PEG-PTX was dissolved in phosphate-buffered saline (PBS; pH 7.4), C57 mouse serum or cholesterol esterase solution and incubated for 48 h at 37°C. The released PTX was separated via ultrafiltration using 100 kDa MWCO filters, and the retained PTX was detected by HPLC at 4, 12, 24 and 48 h incubation.

Cell culture & *in vitro* toxicity

A549 and B16 melanoma cancer cell lines were cultured in DMEM with high glucose supplemented with 10% fatal bovine serum, 100 µg/ml of streptomycin and 100 µg/ml of penicillin. Cells were placed in a humidified atmosphere containing 5% CO_2 at 37°C. The cell medium was changed every other day. For the *in vitro* cell toxicity study, cells were seeded onto a 96-well bottom plate and incubated at 37°C overnight. The cells were then incubated with different concentrations of GO-PEG, GO-PEG-PTX or Taxol (all dissolved in DMEM with high glucose) and blank DMEM with high glucose. After 24 h of incubation, the relative cell viability was measured by MTT assay with Fluoroskan Ascent FL microplate fluorometer and luminometer (Thermo Scientific).

Cellular uptake assay

Both A549 and B16 cells were seeded in 6-well plates. The cells were then exposed to GO-PEG-PTX or Taxol at a range of concentrations (10, 25, 50, 100 µg/ml) for 2 h at 37°C. Cold PBS (20°C pH 7.4) was used to wash the cells in order to remove the drug molecules that were not taken up by those cells. The cells were then digested and collected as the cellular uptake sample, which were centrifuged at 5000 rpm for 5 min. The cell residue was lysed with radioimmunoprecipitation assay buffer in order to release the intracellular drug. Methanol and 20% of trichloroacetic acid were added to the cell digests, followed by centrifugation at 12,000 rpm for 10 min. Supernatants were collected and analyzed by HPLC. The intracellular concentrations of PTX were investigated by HPLC assay using the method described earlier. Twenty microliters of the cell lysate from each sample was taken to determine the total cell protein content using reagent kit (Pierce, USA). The uptake rate was expressed as the amount of PTX associated with a unit weight of cellular protein.

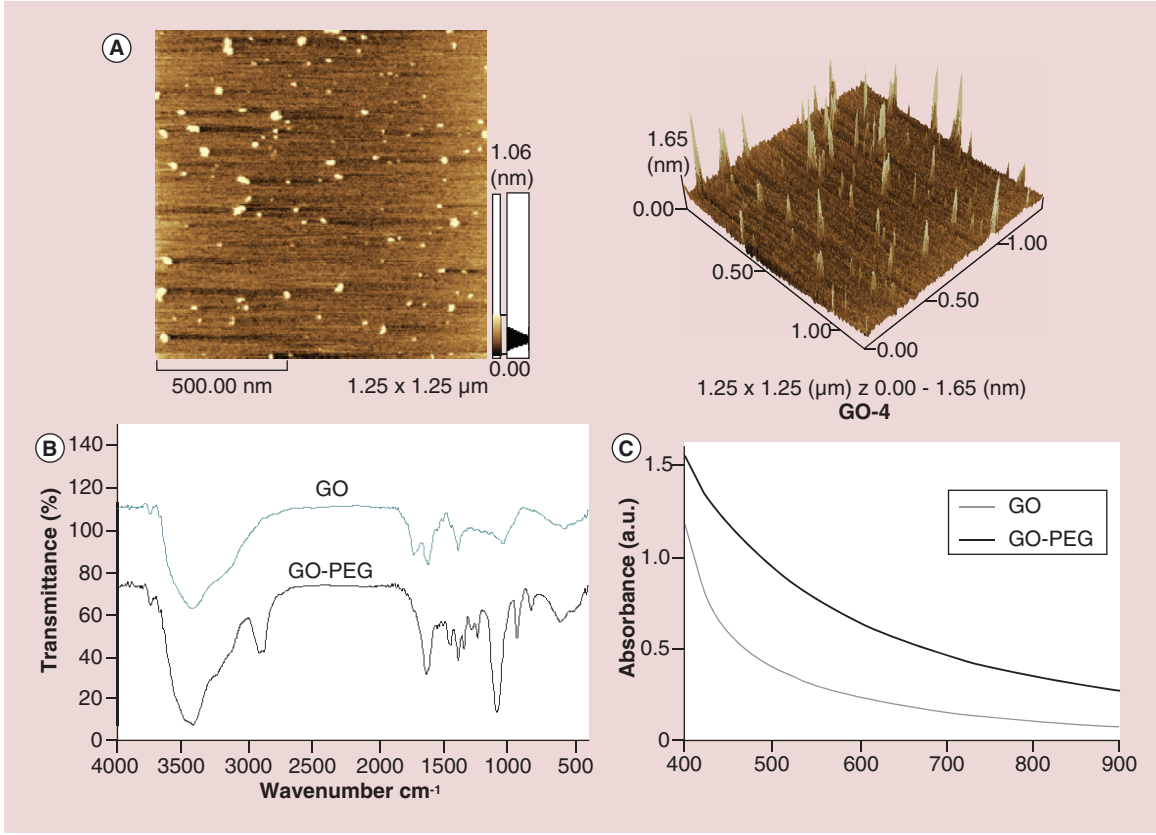

Figure 1. Characterization of graphene oxide-PEG. (A) Atomic force microscopy showed that all shards in the vision were below 50 nm. **(B)** Fourier transform infrared spectra of GO and GO-PEG. **(C)** UV-vis spectra of GO and GO-PEG at the concentration of 0.05 mg/ml.
GO: Graphene oxide.

Pharmacokinetic study

Female Wistar rats (220 ± 20 g) were randomly divided into two groups. The rats received GO-PEG-PTX (GO-PEG-PTX group) or Taxol (Taxol group) via tail vein at a dose equivalent to 2 mg/kg of PTX (n = 5). At 5 min, 10 min, 15 min, 30 min, 1 h, 2 h, 4 h, 8 h, 12 h and 24 h intervals after injection, blood samples were taken and the plasma was separated by centrifugation at 5000 rpm for 5 min. Docetaxel were added to each sample as the internal standard and methanol was used to precipitate the protein followed by centrifugation at 13,000 rpm for 10 min. Supernatants were collected and analyzed by HPLC following the method described above.

Animal model & drug efficacy study

Murine B16 melanoma cancer model was established by subcutaneous injection of about 1.5×10^6 cells in PBS under the right arm of female C57 mice. The mice were used for experiments 14 days after injection (the tumor volume was about 100 mm^3). For the treatment, GO-PEG-PTX or Taxol with a dose equivalent to 4 mg/kg of PTX, GO-PEG and the same volume of saline were injected via caudal vein for three-times (0, 3, 6 days after injection). The tumor size was measured by a caliper every other day and was calculated as V = (tumor length) × (tumor width)^2/2. Relative tumor volumes were calculated as V/V_0 (V_0 was the tumor volume before mice were injected with the formulation). The survival rates of each group were then calculated to construct the survival rate curve.

Biodistribtion study

Female C57 mice bearing B16 tumor (tumor size was about 200 mm^3) were intravenously injected with GO-PEG-PTX or Taxol with a dose equivalent to 50 mg/kg of PTX. The mice were sacrificed at 30 min, 1 h, 4 h, 8 h, 12 h or 24 h after injection. Samples of blood, liver, spleen, lung, kidney and tumor were then collected. The samples of the animals' blood were collected in heparinized tubes. Tissues were isolated, washed with saline and homogenized with twofold volume of 0.9% sodium chloride (g/ml). The blood samples and tissues homogenates were processed and measured by HPLC as described in the pharmacokinetic study.

In vivo toxicity study

Healthy female C57 mice (18~20 g) were randomly assigned into four groups for drug administration. GO-

PEG-PTX or Taxol with a dose equivalent to 4 mg/kg of PTX was intravenously injected into the mice in each group, and the mice in the other two groups were injected with the same volume of GO-PEG or saline via tail vein. The same dose of drug was injected every 5 days after the initial treatment, six-times total. The weight of each mouse was recorded every day and the curve of the bodyweight change was established after the treatment. For histological evaluation, livers and spleens of mice were collected 30 days after the initial treatment and were fixed in 4% v/v paraformaldehyde for 4 days. The samples were taken and stained with hematoxylin and eosin (H & E) for examination by light microscopy (Axiovert 40 CFL, Carl Zeiss; Jena, Germany). For blood chemistry evaluation, blood samples were taken as soon as mice were sacrificed. The blood samples were centrifuged at 5000 rpm and the serum was collected for chemistry analysis.

Results & discussion

Synthesis of GO-PEG-PTX

To improve the solubility and *in vivo* properties of GO, a variety of modifiers were investigated to conjugate to the surface of GO, such as PEG, folic acid, polyethyleneimine, chitosan, etc. [12,13,17,19]. Because PEG has been widely used for improving the water solubility and biocompatibility of many nanomaterials in biomedicine, in this study we chose PEG4000 to improve the solubility and *in vivo* behavior of GO. In brief, GO was first converted to GO-COOH through sonication and carboxylation at the surface of GO. Then NH_2-PEG4k-NH_2 was conjugated with carboxylate groups of GO-COOH via amide bond. The carboxylation was done to convert the esters and epoxides into carboxyl group, by which GO could conjugate with PEG-NH_2. The decoration of GO by PEG significantly improved its solubility both in water and physiological solutions. Fourier transform IR spectra were used to confirm the assigned structure of GO-PEG. The conjugation of PEG with GO-COOH through amide bond formation could be verified by the peak at approximately 2850 cm^{-1}(C-H bond), approximately 1650 cm^{-1} (C=O bond) and approximately 1100 cm^{-1} (C-O bond; Figure 1B). The diameter of each GO-PEG particle was below 50 nm and the thickness of each particle was up to 1.9 nm as observed by atomic force microscopy (Figure 1A). According to the UV-vis spectra, GO-PEG possessed both higher near-infrared and visible absorption than GO did (Figure 1C). The increased optical absorption might be caused by hydrolysis of ester bond and ring-opening of epoxide groups on the surface of GO molecule under the basic synthesis condition during the carboxylation step.

To ensure a proper releasing profile of PTX after intravenous injection, PTX was conjugated to GO-PEG via a cleavable ester bond, which can be hydrolyzed by both chemical and enzymatic pathways (Figure 2A). As shown in Figure 2B, GO-PEG-PTX complex was synthesized by a two-step reaction. First, 2′-O-succinyl-PTX was synthesized, and then 2′-O-succinyl-

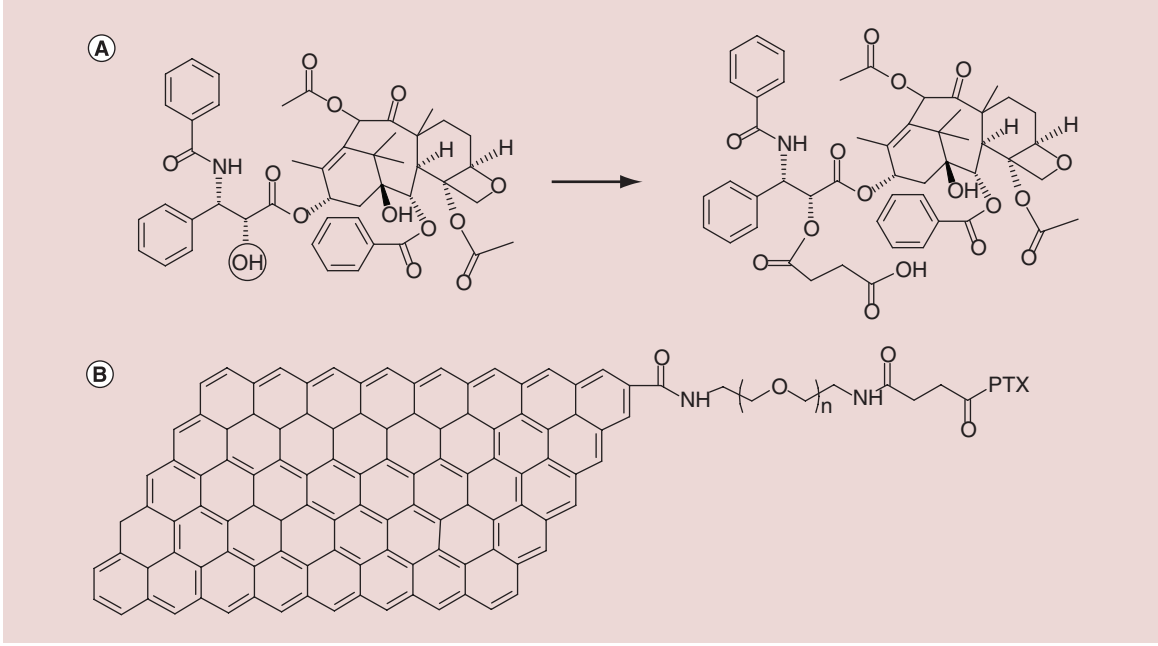

Figure 2. Paclitaxel loading on graphene oxide-PEG. (A) Schematic illustration of paclitaxel modified by succinic anhydride at 2′-OH; **(B)** Schematic illustration showing how graphene oxide was modified by NH_2-PEG4k-$NH_2$and 2′-succinyl paclitaxel was conjugated on graphene oxide-PEG through a cleavable ester bond.

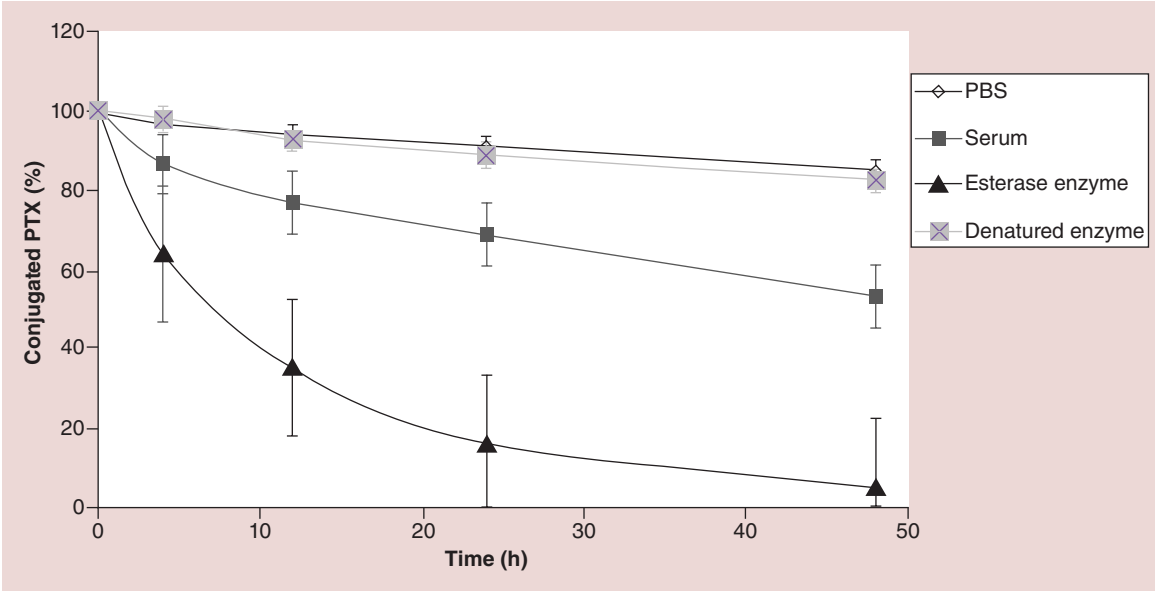

Figure 3. The drug release profile using graphene oxide-PEG-paclitaxel in phospate-buffered saline solution, C57 mouse serum, esterase enzyme solution and heat denatured enzyme solution after 48 h of incubation with phospate-buffered saline and serum, respectively, at 37°C. The retained paclitaxel was collected by filtration and detected by HPLC.

PTX was conjugated to GO-PEG. The synthesis of 2′-O-succinyl-PTX was carried out according to the previously reported methods [41,50–52]. As described in Figure 2A, the PTX molecule was first linked by its 2′-hydroxyl terminus with succinic anhydride. Thin-layer chromatography analysis was used for detecting whether free PTX was fully converted to the resultant. The unreacted succinic anhydride turned into water soluble succinic acid after stirring at 60°C for 1 h. The desired compound was obtained by purification using a silica gel column. After that, modified PTX was coupled to the terminal amine group of the PEG previously being attached on the surface of GO molecule through amide bond [50]. As a standard reaction of forming amide bond, 2′-O-succiyl-PTX and GO-PEG were dissolved in water/DMSO (1:1) mixed solvent and EDC-HCL and NHS were added as catalysts. After dialysis in DMSO and water respectively, the purified GO-PEG-PTX was analyzed by HPLC method to confirm the successful synthesis. According to the HPLC result, approximately 0.51 mg of PTX was conjugated on 1 mg of GO-PEG. Different from blank PTX, GO-PEG-PTX exhibited improved solubility both in water and in saline. *In vitro* release study at 37°C indicated that GO-PEG-PTX displayed excellent stability in PBS solution, in which only very low proportion of PTX was released from GO-PEG-PTX complex within 48 h (Figure 3). The release rate of PTX in C57 mice serum was faster than that in PBS (about 30% of total PTX was released within 24 h). What is more, the release rate of PTX in esterase enzyme solution was much faster than those in PBS and serum. While in denatured enzyme solution, the release rate was similar with that in PBS. So the cleavage of ester bond in serum could be ascribed to the existence of esterase enzyme. Importantly, the relatively moderate release rate might ensure that PTX loaded onto GO-PEG would reach the target tissue and then release PTX to exert therapeutic effect.

In vitro investigation of GO-PEG-PTX

Cytotoxicity of GO-PEG-PTX was investigated using MTT assay with A549 and B16 cancer cell lines. As indicated in Figure 4, GO-PEG-PTX exhibited approximately similar cytotoxic efficacy to that exhibited by Taxol at relatively high concentrations. No obvious cytotoxicity of plain GO-PEG was found during the experiments, even at high concentrations. These results indicated that loading PTX in GO-PEG did not significantly interfere or reduce cytotoxicity of PTX against cancer cells.

We then further investigated the cellular uptake of GO-PEG-PTX using A549 and B16 cell lines. Some previous research investigations have employed fluorescent or radioactive materials to tag GO molecules in order to monitor their dynamics following cellar uptake [34,50]. In this study, we used HPLC to investigate the cellular uptake rate because the linear chain of NH_2-PEG4k-NH_2 did not have much room for conjugating the fluorescent material, especially when two terminals of PEG were occupied by both GO and PTX. HPLC method was established to monitor the intracellular drug contents. It was shown in Figure 5 that the

intracellular concentration of drug using GO-PEG-PTX was slightly lower than that of Taxol at low doses. However, when the drug concentration was increased the intracellular drug content almost reached the same level of that seen by Taxol. Both A549 and B16 cell lines shared the same tendency. The cellular uptake results and the cytotoxicity investigation suggested that the *in vitro* anti-cancer ability of GO-PEG-PTX was comparable to that of Taxol at the relatively high concentrations used. However, the *in vitro* anticancer ability of GO-PEG-PTX was lower than that of Taxol at the relatively low doses. The previous study of Liu *et al.* showed that cytotoxicity of PTX conjugated to SWNTs was relatively lower than that of Taxol at certain drug dose range (10~100 μg/ml) [50]. The low cellular uptake rate of the PTX on GO-PEG might be attributed to conjugation between PTX and GO-PEG. This was confirmed previously by Chang *et al.* who have reported that GO alone could hardly be taken up by cancer cells [7]. However, GO-PEG could enter the cells through energy required endocytosis mechanism [10,38]. Thus when conjugated with GO-PEG, PTX was able to enter the cancer cells along with GO-PEG-PTX complex through endocytosis. Although the conjugation with GO hindered the immediate uptake of PTX by the cells, the long blood circulation time offered by conjugating the drug to GO-PEG after *in vivo* treatment was highly advantageous at enhancing the anticancer efficacy of PTX. Using this strategy, PTX administration as GO-PEG-PTX may result in higher drug bioavailability and enhanced antitumor effect.

Pharmacokinectic investigation of GO-PEG-PTX

In order to understand the pharmacokinetics of GO-PEG-PTX, we used HPLC assay to measure PTX concentration in plasma at different time intervals after intravenous injection of the formulations into Wistar rats via tail vein (2 mg/kg). Blood was collected at different time points after injection. The time–concentration curves of GO-PTX-PEG and Taxol both exhibited a standard two-compartment model. As shown in Figure 6, the elimination speed of PTX was relatively rapid both in GO-PEG-PTX and Taxol group. Compared with Taxol, longer second phase blood circulation half-time, higher bioavailability and lower clearance rate were observed for GO-PEG-PTX. The underlying reason was that some time is needed for the cleavage of ester linkage between PTX and GO-PEG to occur [53].

Biodistribution & *in vivo* toxicity investigations of GO-PEG-PTX

To further evaluate the tumor targeting ability of GO-PEG-PTX, we studied tissue distribution of GO-PEG-PTX and Taxol in B16 melanoma cancer bearing C57 mice. The tissue distribution of GO-PEG-PTX and Taxol were measured at 30 min, 1 h, 4 h, 8 h, 12 h and 24 h after injecting GO-PEG-PTX or Taxol via tail veins of B16 tumor-bearing mice. At predetermined time points, the blood samples were collected and the animals were sacrificed. Tissues including hearts, livers, spleens, lungs and kidneys were isolated immediately. Plasma or tissue homogenates were extracted by methanol, and then quantitative measurement of PTX was done by HPLC. As shown in Figure 7, after intravenous administration of GO-PEG-PTX, peak concentrations of PTX in tumor were achieved within 4 h (14.2%), which was significantly higher than that of Taxol group. The concentration of PTX remained relatively high even at 24 h (2%) after administration. For other tissues (Figure 8), the liver and kidney reached the highest concentration within 0.5 h (28 and 16%), decreasing gradually over time. The highest concentration in spleen and lung were achieved within 1 h (32 and 6%, respectively). After 24 h of treatment, PTX in liver and spleen

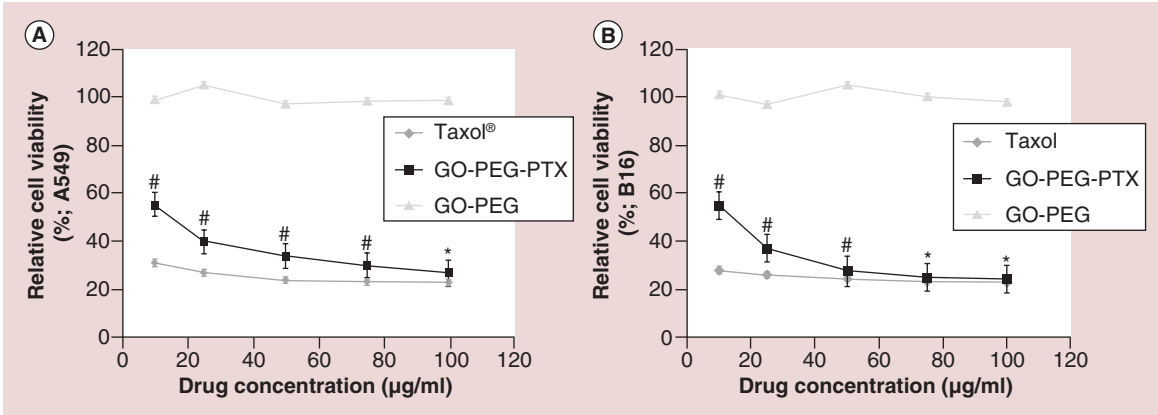

Figure 4. Comparison of cell survival curves for A549 and B16 cells incubated with graphene oxide-PEG, graphene oxide-PEG-paclitaxel or Taxol® for 48 h. The cytotoxicity of graphene oxide-PEG-paclitaxel approximated to that of Taxol at high drug concentrations.
$^{\#}p \leq 0.01$; $^{*}p \leq 0.05$.

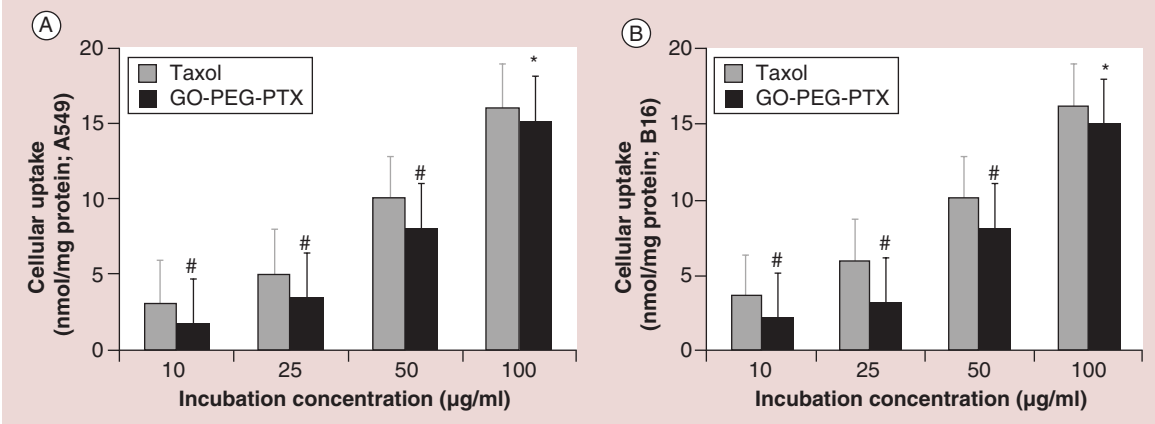

Figure 5. Comparison of the cellular uptake of graphene oxide-PEG-paclitaxel and Taxol® using B16 and A549 cell lines, which generally demonstrated approximate uptake level of graphene oxide-PEG-paclitaxel and Taxol at the concentration of 100 μg/ml. (A) *In vitro* cellular uptake of GO-PEG-PTX and Taxol in A549 cells using a range of drug concentrations (10, 25, 50 and 100 μg/ml). Taxol exhibited relatively higher uptake rate at low drug concentrations, but the difference between Taxol and GO-PEG-PTX decreased along with the increase in drug concentration; they nearly reached the same uptake at 100 μg/ml ($^{\#}p \leq 0.01$, $^{*}p \leq 0.05$). **(B)** *In vitro* cellular uptake of GO-PEG-PTX and Taxol in B16 cells using a range of drug concentrations (10, 25, 50 and 100 μg/ml); the two formulations shared the same trend with that in A549 cells ($^{\#}p \leq 0.01$, $^{*}p \leq 0.05$).
GO: Graphene oxide; PTX: Paclitaxel.

remained at moderate levels (7 and 6%, respectively).

By contrast, after intravenous administration of Taxol, peak concentrations of PTX in tumor were achieved within 8 h (4%), and PTX decreased significantly to a very low concentration in tumor at 24 h postinjection. In the case of other organs (Figure 8), at 0.5 h, PTX was widely distributed in liver (56%), kidney and lung with negligible concentrations being detected in the tumor tissue (0.08%). The drug concentration in liver, lung and kidney reached the highest within 0.5 h, and then decreased gradually over time. The concentration of PTX in spleen remained relatively low throughout the detection period, which reached the highest amount at 12 h (2%). PTX in all tissues were almost cleared completely at 24 h except liver (4%).

The results of tissue distribution of GO-PEG-PTX and Taxol reflected the tumor-treatment efficacy and main organ accumulation of the two formulations. By conjugating with GO-PEG, PTX exhibited a significantly different *in vivo* distribution. PTX given as GO-PEG-PTX showed higher blood concentration than Taxol over the whole time course examined, which was consistent with the pharmacokinetic investigation. The distinct difference between GO-PEG-PTX and plain PTX in physiological solutions could be attributed to the prolonged blood circulation. Another obvious difference in tissue distribution of PTX was the concentration in spleen. Much higher concentration was found in GO-PEG-PTX group compared with that in the Taxol group. After injection of GO-PEG-PTX, the PTX concentrations were 27-, 25- and 14-times higher than that of Taxol at 1, 4 and 8 h, respectively. It was previously reported that graphene as well as SWNTs have higher accumulating capacity in RES organs such as liver and spleen [38,39,50,54,55]. Liu *et al.* proved that the uptake of drug-macromolecular complex such as PTX-SWNTs by RES organs could serve as a scavenger system to metabolize and eliminate toxic drugs as well as carriers. Therefore, when we utilize GO as a drug carrier, the toxicity in those organs must be considered. Some reports announced that unmodified GO may induce some adverse effects [37,56,57]. However, Liu *et al.* demonstrated that no noticeable organ damage or inflammation was observed after intravenous injection of GO-PEG into mice at a dose of 20 mg/kg [58]. In this study, we have also investigated the *in vivo* toxicity of GO-PEG-PTX and made a comparison with that of Taxol, plain GO-PEG and saline. After intravenous administration of those four formulations, the weight of each C57 mouse was recorded every day. According to the results obtained, no significant bodyweight change was observed in each group 30 days after the treatment (Figure 9B). Blood chemistry analysis was performed 30 days after the first injection of different formulation. No obvious differences between the four groups were found (Figure 9A), indicating that GO-PEG-PTX did not cause any detectable physiological damage to the liver at the given dose. Meanwhile, as displayed in Figure 9C, the immunohistochemistry analysis of liver and spleen separated from the mouse in each group 30 days after the treatment did not show any inflammation or pathological changes. According to these results, GO-PEG-PTX has shown to be safe for *in vivo* administration at the dose of 2 mg/kg, and its accumulation in RES organs such as liver and

spleen did not seem to affect the health condition of C57 mice within the time course of the investigation. Although the investigations above and other researchers' study proved the safety of the nanocarrier, Singh *et al.* have reported that atomically thin GO sheets could induce thrombus [59]. And amine-modified graphene can avoid the aggregatory response in platelets [60]. The toxicity study over 30 days is not sufficient to prove the long-term safety of GO-PEG-PTX. As a consequence, the long-term behavior study and more comprehensive investigations of GO-PEG-PTX are needed to further validate the *in vivo* safety of this formulation.

It was clearly shown in our data that GO-PEG-PTX exhibited much higher PTX uptake rate in tumor tissue than that of Taxol by about 5.5-times (1 h), 3.5-times (4 h), 3.3-times (8 h) and 2.8-times (12 h; Figure 7). Even at 24 h after injection, PTX concentration of GO-PEG-PTX in tumor remained above 2% (i.e., 12-times higher than that of Taxol). The enhanced permeability and retention effects of GO could be the main reason of the significantly increased PTX distribution in tumor using GO-PEG-PTX. It was believed that the leaky and tortuous vasculatures of tumor tissue might prefer to withhold nanosize materials such as graphene and SWNTs. The tumor targeting ability of GO has been shown to be stronger than that of SWNTs because of their difference in geometrical structure [54,61,62]. The longer residence time in the blood of the nanoconjugate may contributed to the higher uptake rate but not the most important factor. Even though the biodistribution of GO-PEG, of which had a long-term accumulation process lasting for several weeks [38,50], PTX loading on GO-PEG was metabolized and excreted quickly. The difference between the tissue distribution of GO-PEG and GO-PEG-PTX were possibly caused by the cleavage of the ester linkage between PTX and GO-PEG after injection into the animals. Because the same result has also been reported in the biodistribution study of PTX-SWNTs [50]. It was believed that the ester linkage was cleaved by carboxylesterases mostly in the liver [50,53,63,64]. In a word, our study indicated that GO-PEG-PTX exhibited much longer blood circulation time

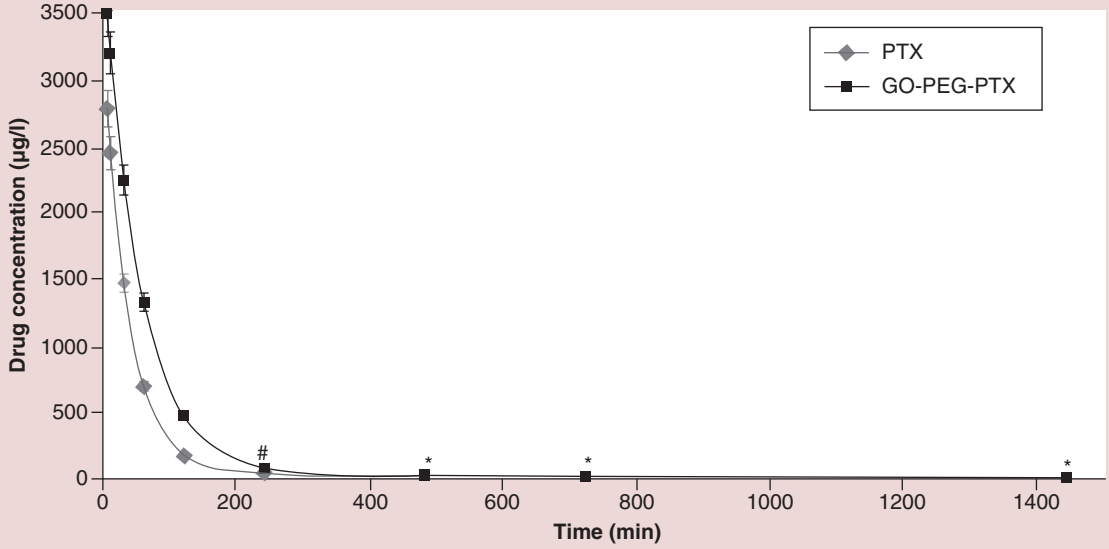

Parameters	GO-PEG-PTX	Taxol®
$T_{1/2}$ (h)	13.9	11.51
K (1/h)	0.23	0.17
$AUC_{0-24\,h}$ (μg/1/h)	4409.3	2617
CL (1/h)	0.017	0.031

Figure 6. The blood circulation curve of Taxol® and graphene oxide-polyethylene glycol-paclitaxel. The pharmacokinetic models of both Taxol and graphene oxide-polyethylene glycol-paclitaxel followed the two compartment model. The data inserted are the second-phase blood circulation half-time ($T_{1/2}$), K, AUC within 24 h ($AUC_{0-24\,h}$) and clearance rate.
$^{\#}p \leq 0.01$, $^{*}p \leq 0.05$.
$AUC_{0-24\,h}$: Area under concentration–time curve within 24 h; GO: Graphene oxide; K: Elimination rate constant; PTX: Paclitaxel; T1/2: Second-phase blood circulation half-time.

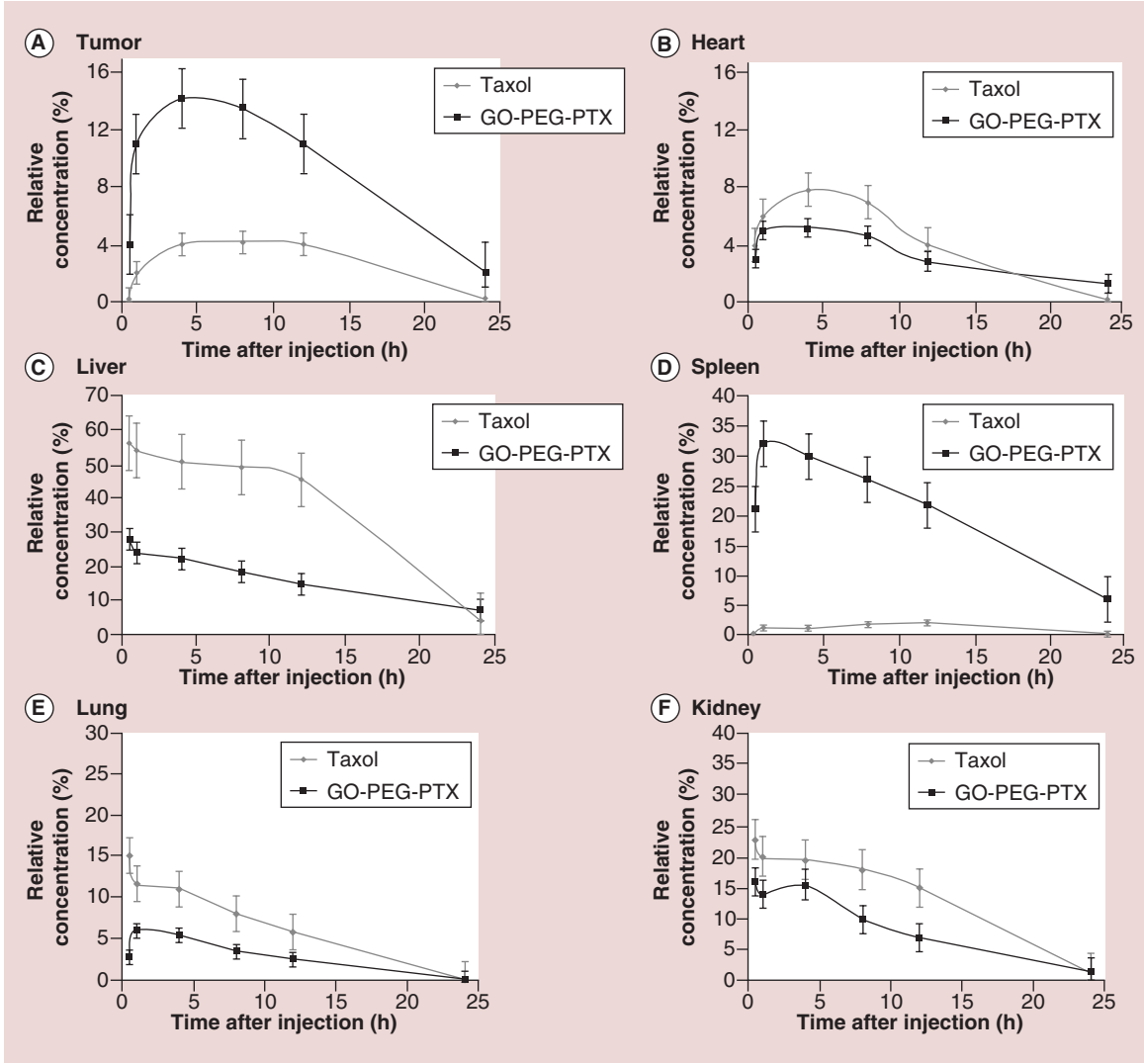

Figure 7. Concentration–time curves of PTX in different tissues. Relative concentration-time curves of graphene oxide-PEG-PTX and Taxol® in different tissues of C57 mice bearing B16 tumors at 0.5, 1, 4, 8, 12 and 24 h after intravenous injection (n = 5 for each group at each time point), which were significantly different among all groups ($p \leq 0.05$).

and thus much better tumor uptake rate than the formulation of Taxol. These results implied that a lower dosage of GO-PEG-PTX might achieve the same anticancer efficacy as Taxol did. As a consequence, our novel conjugate would reduce the toxicity and side effects of PTX in normal organs, hence possibly offering more desirable characteristics and better safety profile compared with the market available formulation of PTX (Taxol).

In vivo tumor-suppressing investigation of GO-PEG-PTX

In order to investigate the *in vivo* cancer suppressing efficacy of GO-PEG-PTX and compare to that of Taxol, B16 murine melanoma cancer animal model was established for the experiments. Female C57 mice bearing subcutaneously implanted B16 tumors were intravenously injected with GO-PEG-PTX or Taxol at the equivalent dosage of PTX for three-times (0, 3, 6 days after injection), where 0 day refers to the day of injecting PTX formulations for the first time. Two weeks after injection, the tumor volume and survival condition were recorded every day. The results of tumor growth speed showed that the injection of GO-PEG-PTX induced significant tumor inhibition as compared with that of Taxol (Figure 10A). Taxol can only suppress tumor growth at a relatively moderate rate. The tumor growth speed showed no difference between blank GO-PEG group and saline group, which indicated that the blank GO-PEG itself did not have any anticancer efficacy. The survival time of each group also shared the same tendency with the result of tumor growth speed (Figure 10B). Mice in GO-PEG-PTX group had the longest survival time. The survival time of mice in Taxol

group was less than that of GO-PEG-PTX group, but was longer than those of GO-PEG and saline groups.

It was shown that PTX loading on GO-PEG possessed significantly improved anticancer efficacy compared with Taxol, which was proved by slowing down the tumor growth and the prolonging survival time. The significantly higher tumor-suppressing rate of GO-PEG-PTX might be ascribed to its much higher tumor uptake compared with that of Taxol, which was verified in our biodistribution study. No enhanced tumor-suppressing effect or longer survival time of mice after blank GO-PEG treatment was observed, indicating that the GO-PEG material only played a role of drug carrier without eliciting any noticeable anticancer efficacy. However, Arya *et al.* have reported that carbon nanostructures such as GO and SWNTs can enhance the sensitivity of lung cancer cells to PTX when carbon nanostructures and PTX were incubated with cells together. Their *in vitro* study indicated that GO and SWNTs had the ability to generate reactive oxygen species, which was crucial for PTX induced cell death, as potential cotherapeutics for PTX [65]. We believe that further *in vivo* investigations are needed to illuminate the anticancer ability of blank GO-PEG using different cancer models, and more prolonged course of therapy and different experimental conditions.

To the best of our knowledge, using GO as a carrier for PTX through covalent conjugation to achieve *in vivo* therapeutic effects is a novel approach to improve the physiological solubility, bioavailability and tumor targeting ability of PTX. The unique features of the surface of GO facilitates the loading of other anticancer drugs or photosensitizers [10,14,66], which might cause additive or synergistic effects along with the anticancer agent, and the GO-drug complex can also absorb near infrared light to achieve photothermal

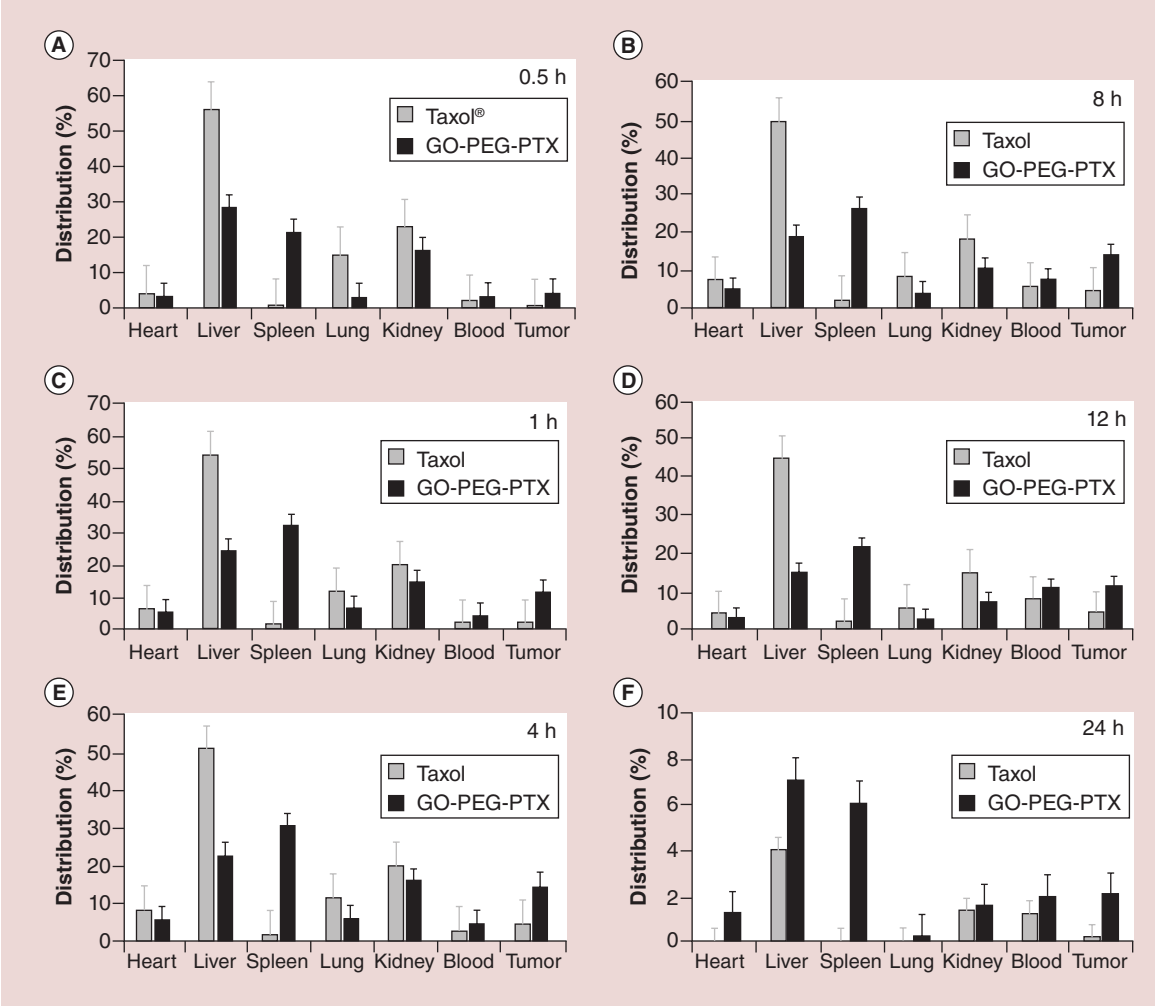

Figure 8. Tissue distribution of graphene oxide-PEG-paclitaxel and Taxol®. Tissue distribution of graphene oxide-polyethylene glycol-paclitaxel and Taxol in C57 mice bearing B16 tumors at 0.5, 1, 4, 8, 12 and 24 h after intravenous injection (n = 5 for each group at each time interval), which were significantly different among all groups ($p \leq 0.05$). GO: Graphene oxide; PTX: Paclitaxel.

therapy over tumor tissue [22,34]. Those investigations can be carried out in the future to improve GO-PTX system starting from the highly promising findings established in our present investigation.

We have selected B16 melanoma model in the experiment because in our laboratory it is commonly used in anticancer research, so we have a lot of experience with it. Moreover, GO-PEG-PTX exhibited better anticancer efficacy than PTX against this cancer model. However, we feel confident that following the presented findings in this manuscript we will continue to investigate the anticancer efficacy of GO-PEG-PTX using different cancer models.

Even though GO-based nanoconjugate we investigated have a lot of advantages in anticancer efficacy and in vivo safety, it still has limitation and lack of preclinical and clinical investigation compared with the US FDA approved anticancer drug, nab-Taxol. Further investigations and comparison will be carried out to state that the nanoconjugate is amenable to improvement and modification due to the advances in GO possesses.

Conclusion & future perspective

In summary, we loaded PTX on GO-PEG carrier system through covalent conjugation, and studied the therapeutic effects of GO-PEG-PTX *in vitro* and *in vivo*. Compared with Taxol, GO-PEG-PTX exhibited better tumor-suppressing efficacy due to the higher uptake rate in tumor tissue. No obvious *in vivo* toxicity or tissue damage was found in mice after intravenous injection of GO-PEG-PTX for 30 days. All findings in this study indicated that PEGylated GO is an excellent nanocarrier for PTX for cancer targeting. However, GO still has several issues in need for further investigations. In the future the merit of GO may possibly have compared with other nanomaterials, the long-term *in vivo* safety, LD 50 of the conjugate, comprehensive comparison with the FDA approved nab-PTX will be carried out. Moreover, using the nanoconjugate to load other chemical anticancer drugs and functional genes, as well as photothermal and photodynamical therapies may enhance the efficacy of PTX. Thus, the research focus on combining two or more

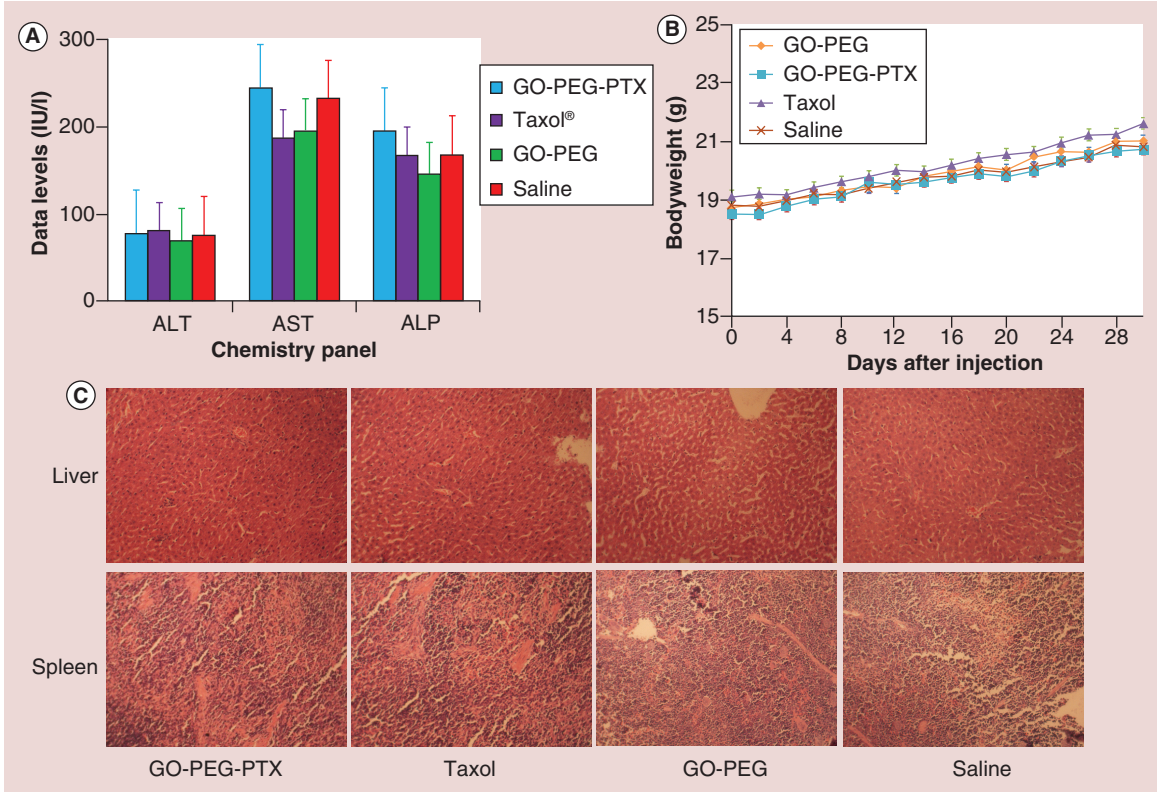

Figure 9. Relative low *in vivo* toxicity and tissue damage using graphene oxide-polyethylene glycol-paclitaxel.
(A) Blood chemistry analysis of mice treated with graphene oxide-polyethylene glycol-paclitaxel (GO-PEG-PTX), Taxol, GO-PEG and saline for 30 days, which included ALT, AST and ALP. These findings indicate no deviant changes in GO-PEG-PTX group compared with other groups. **(B)** Bodyweight changing curves of C57 mice treated with GO-PEG, GO-PEG-PTX, Taxol® or saline for 30 days. No obvious abnormal weight changes were observed between the four groups. **(C)** Histological evaluation of liver and spleen collected from the mouse along with collecting the blood for paraffin section and H&E staining. No obvious tissue damage was observed in the liver or the spleen when GO-PEG-PTX was injected (magnification 200×).
GO: Graphene oxide; PTX: Paclitaxel.

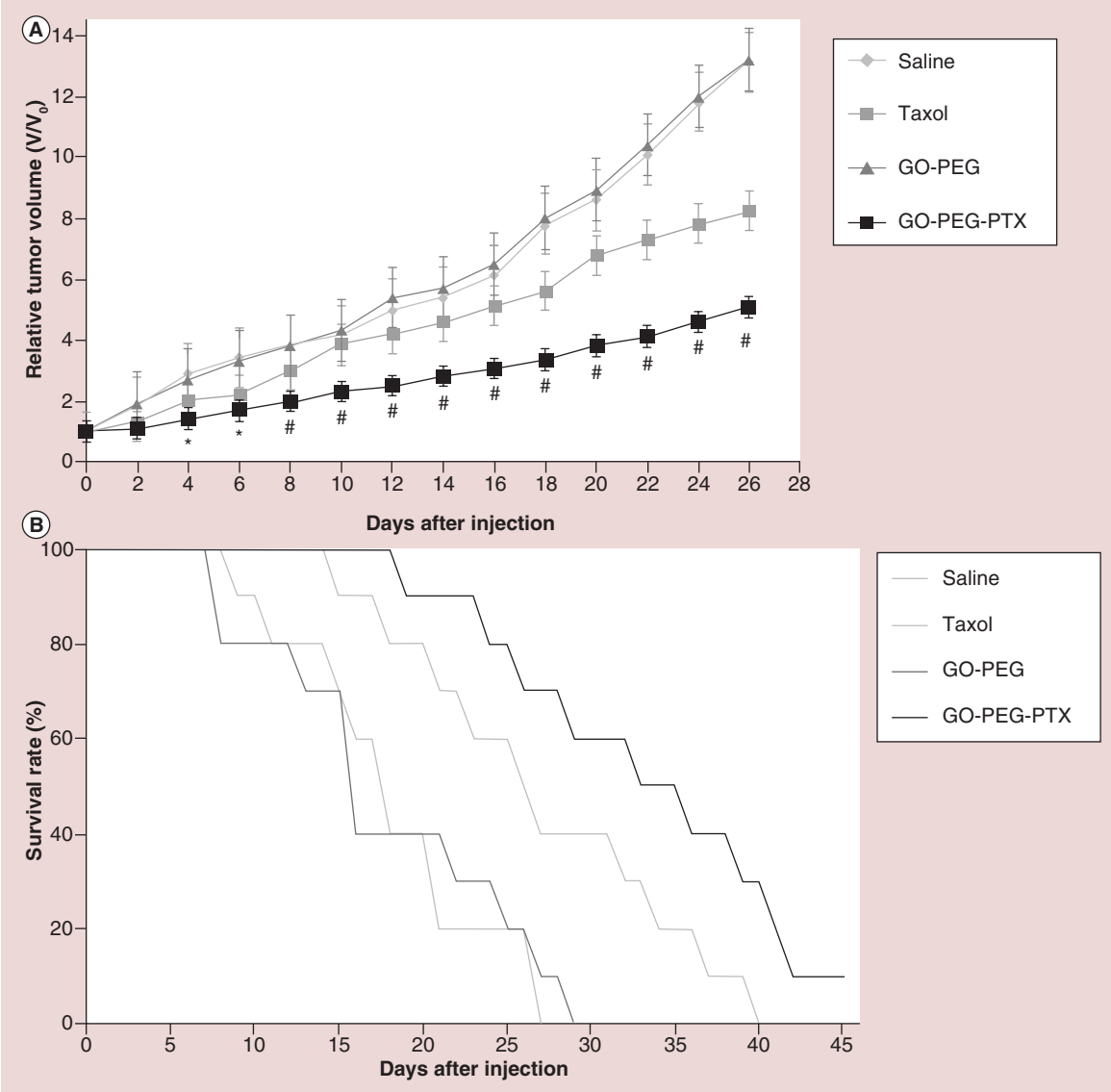

Figure 10. The tumor-suppressing efficacy of graphene oxide-polyethylene glycol-paclitaxel after intravenous injecting into the cancer bearing mice; each group consisted of ten mice. (A) The changing rate of relative tumor volume on tumor-bearing mice after injecting the same PTX dose using GO-PEG-PTX or Taxol®, along with the same volume of GO-PEG and saline (#$p \leq 0.01$, *$p \leq 0.05$; GO-PEG-PTX comparing to Taxol). **(B)** The survival time of tumor-bearing mice after injecting GO-PEG-PTX, Taxol, GO-PEG or saline.
GO: Graphene oxide; PTX: Paclitaxel

different anticancer strategies to achieve synergistic effect of GO may have a good perspective. Being a promising nanocarrier for PTX, GO has a brilliant future in anticancer application. We also believe GO can attract more novel researches in cancer therapy biomedical imaging and biological sensing because of its unique properties.

Financial & competing interests disclosure

The authors are grateful for the financial support from the University of Central Lancashire, United Kingdom and UClan Biomedical Technology (Shenzhen) Ltd. The authors have no other relevant affiliations or financialinvolvement with any organization or entity with a financial interest in or financial conflict with the subject matter or materials discussed in the manuscript apart from those disclosed.

No writing assistance was utilized in the production of this manuscript.

Ethical conduct of research

The authors state that they have obtained appropriate institutional review board approval or have followed the principles outlined in the Declaration of Helsinki for all human or animal experimental investigations. In addition, for investigations involving human subjects, informed consent has been obtained from the participants involved.

Executive summary

Merits of PEGylated graphene oxide applied in anticancer therapy field

- Owing to the good water solubility, highly dispersed ability, high drug-loading efficacy and passive tumor-targeting ability, graphene oxide (GO) can be used as a carrier to deliver certain drugs into tumor tissues.
- PEGylation of GO can improve its solubility in saline and biocompatibility. The obtained GO-PEG can be utilized for biomedical applications.

Demand for improvement using paclitaxel in anticancer chemotherapy strategy

- The side effects, toxicity and severe anaphylaxis of paclitaxel (PTX) injections used in clinic limit their application.
- PTX was covalently conjugated onto GO-PEG to optimize the solubility and biocompatibility. GO-PEG-PTX can delivery PTX molecules to tumor tissues resulting the improved therapeutic effect.

***In vivo* investigation**

- GO-PEG-PTX exhibited prolonged blood circulation time, much higher tumor distribution and better anticancer efficacy compared with Taxol®.
- GO-PEG-PTX did not show any obvious or severe in vivo toxicity in the current investigation.

Conclusion & future perspective

- PEGylated graphene oxide is an excellent nanocarrier to load PTX for cancer targeting.
- More detailed *in vivo* toxicity investigation will be carried out to improve its safety.
- Further investigations in the future will include other anticancer drugs and differently surface-engineered graphene oxide.

References

Papers of special note have been highlighted as:
•• of considerable interest

1 Geim AK, Novoselov KS. The rise of graphene. *Nat. Mater.* 6(3), 183–191 (2007).

2 Hass J, De Heer W, Conrad E. The growth and morphology of epitaxial multilayer graphene. *J. Phys. Condens. Matter* 20(32), 323202 (2008).

3 Huang X, Yin Z, Wu S *et al.* Graphene-based materials: synthesis, characterization, properties, and applications. *Small* 7(14), 1876–1902 (2011).

4 Wang Y, Li Z, Wang J, Li J, Lin Y. Graphene and graphene oxide: biofunctionalization and applications in biotechnology. *Trends Biotechnol.* 29(5), 205–212 (2011).

5 Li X, Wang X, Zhang L, Lee S, Dai H. Chemically derived, ultrasmooth graphene nanoribbon semiconductors. *Science* 319(5867), 1229–1232 (2008).

6 Loh KP, Bao Q, Eda G, Chhowalla M. Graphene oxide as a chemically tunable platform for optical applications. *Nat. Chem.* 2(12), 1015–1024 (2010).

7 Chang Y, Yang ST, Liu JH *et al.* In vitro toxicity evaluation of graphene oxide on A549 cells. *Toxicol. Lett.* 200(3), 201–210 (2011).

8 Ali-Boucetta H, Bitounis D, Raveendran-Nair R, Servant A, Van Den Bossche J, Kostarelos K. Purified graphene oxide dispersions lack *in vitro* cytotoxicity and *in vivo* pathogenicity. *Adv. Healthc. Mater.* 2(3), 433–441 (2013).

9 Feng L, Liu Z. Graphene in biomedicine: opportunities and challenges. *Nanomedicine* 6(2), 317–324 (2011).

•• **First paper reported that modified graphene molecule can load water-insoluble anticancer drugs through noncovalent conjugation.**

10 Liu Z, Robinson JT, Sun X, Dai H. PEGylated nanographene oxide for delivery of water-insoluble cancer drugs. *J. Am. Chem. Soc.* 130(33), 10876–10877 (2008).

11 Sun X, Liu Z, Welsher K *et al.* Nano-graphene oxide for cellular imaging and drug delivery. *Nano Res.* 1(3), 203–212 (2008).

12 Zhang L, Xia J, Zhao Q, Liu L, Zhang Z. Functional graphene oxide as a nanocarrier for controlled loading and targeted delivery of mixed anticancer drugs. *Small* 6(4), 537–544 (2010).

13 Feng L, Zhang S, Liu Z. Graphene based gene transfection. *Nanoscale* 3(3), 1252–1257 (2011).

14 Tian B, Wang C, Zhang S, Feng L, Liu Z. Photothermally enhanced photodynamic therapy delivered by nano-graphene oxide. *ACS Nano* 5(9), 7000–7009 (2011).

15 Yang X, Zhang X, Ma Y, Huang Y, Wang Y, Chen Y. Superparamagnetic graphene oxide–Fe3O4 nanoparticles hybrid for controlled targeted drug carriers. *J. Mater. Chem.* 19(18), 2710 (2009).

16 Yang X, Zhang X, Liu Z, Ma Y, Huang Y, Chen Y. High-efficiency loading and controlled release of doxorubicin hydrochloride on graphene oxide. *J. Phys. Chem. C* 112(45), 17554–17558 (2008).

17 Rana VK, Choi M-C, Kong J-Y *et al.* Synthesis and Drug-delivery behavior of chitosan-functionalized graphene oxide hybrid nanosheets. *Macromol. Mater. Eng.* 296(2), 131–140 (2011).

18 Yang X, Wang Y, Huang X *et al.* Multi-functionalized graphene oxide based anticancer drug-carrier with dual-targeting function and pH-sensitivity. *J. Mater. Chem.* 21(10), 3448 (2011).

19 Bao H, Pan Y, Ping Y *et al.* Chitosan-functionalized graphene oxide as a nanocarrier for drug and gene delivery. *Small* 7(11), 1569–1578 (2011).

20 Liu K, Zhang JJ, Cheng FF, Zheng TT, Wang C, Zhu JJ. Green and facile synthesis of highly biocompatible graphene

nanosheets and its application for cellular imaging and drug delivery. *J. Mater. Chem.* 21(32), 12034–12040 (2011).

21 Pan Y, Bao H, Sahoo NG, Wu T, Li L. Water-soluble poly(N-isopropylacrylamide)-graphene sheets synthesized via click chemistry for drug delivery. *Adv. Funct. Mater.* 21(14), 2754–2763 (2011).

22 Yang K, Zhang S, Zhang G, Sun X, Lee ST, Liu Z. Graphene in mice: ultrahigh in vivo tumor uptake and efficient photothermal therapy. *Nano Lett.* 10(9), 3318–3323 (2010).

23 Yang K, Hu L, Ma X *et al.* Multimodal imaging guided photothermal therapy using functionalized graphene nanosheets anchored with magnetic nanoparticles. *Adv. Mater.* 24(14), 1868–1872 (2012).

24 Wang Y, Li Z, Hu D, Lin C-T, Li J, Lin Y. Aptamer/graphene oxide nanocomplex for in situ molecular probing in living cells. *J. Am. Chem. Soc.* 132(27), 9274–9276 (2010).

25 Gollavelli G, Ling Y-C. Multi-functional graphene as an *in vitro* and *in vivo* imaging probe. *Biomaterials* 33(8), 2532–2545 (2012).

26 Tang LaL, Wang J, Loh KP. Graphene-based SELDI probe with ultrahigh extraction and sensitivity for DNA oligomer. *J. Am. Chem. Soc.* 132(32), 10976–10977 (2010).

27 He S, Song B, Li D *et al.* A graphene nanoprobe for rapid, sensitive, and multicolor fluorescent DNA analysis. *Adv. Funct. Mater.* 20(3), 453–459 (2010).

28 Zhao XH, Ma QJ, Wu XX, Zhu X. Graphene oxide-based biosensor for sensitive fluorescence detection of DNA based on exonuclease III-aided signal amplification. *Anal. Chim. Acta* 727, 67–70 (2012).

29 Dong H, Zhang J, Ju H *et al.* Highly sensitive multiple microRNA detection based on fluorescence quenching of graphene oxide and isothermal strand-displacement polymerase reaction. *Anal. Chem.* 84(10), 4587–4593 (2012).

30 Zhu L, Luo L, Wang Z. DNA electrochemical biosensor based on thionine-graphene nanocomposite. *Biosens. Bioelectron.* 35(1), 507–511 (2012).

31 Akhavan O, Ghaderi E, Rahighi R. Toward single-DNA electrochemical biosensing by graphene nanowalls. *ACS Nano* 6(4), 2904–2916 (2012).

32 Jung JH, Cheon DS, Liu F, Lee KB, Seo TS. A Graphene Oxide Based Immuno-biosensor for Pathogen Detection. *Angew. Chem. Int. Ed.* 49(33), 5708–5711 (2010).

33 Loh KP, Bao Q, Ang PK, Yang J. The chemistry of graphene. *J. Mater. Chem.* 20(12), 2277–2289 (2010).

34 Zhang W, Guo Z, Huang D, Liu Z, Guo X, Zhong H. Synergistic effect of chemo-photothermal therapy using PEGylated graphene oxide. *Biomaterials* 32(33), 8555–8561 (2011).

35 Yang K, Wan J, Zhang S, Tian B, Zhang Y, Liu Z. The influence of surface chemistry and size of nanoscale graphene oxide on photothermal therapy of cancer using ultra-low laser power. *Biomaterials* 33(7), 2206–2214 (2012).

36 Zhang S, Yang K, Feng L, Liu Z. *In vitro* and *in vivo* behaviors of dextran functionalized graphene. *Carbon* 49(12), 4040–4049 (2011).

37 Wang K, Ruan J, Song H *et al.* Biocompatibility of graphene oxide. *Nanoscale Res. Lett.* 6(8), (2011).

•• **Symstematically investigates the *in vivo* pharmacokinetics, long-term biodistribution and toxicity of graphene oxide-PEG.**

38 Yang K, Wan J, Zhang S, Zhang Y, Lee ST, Liu Z. In vivo pharmacokinetics, long-term biodistribution, and toxicology of PEGylated graphene in mice. *ACS Nano* 5(1), 516–522 (2010).

39 Liu Z, Davis C, Cai W, He L, Chen X, Dai H. Circulation and long-term fate of functionalized, biocompatible single-walled carbon nanotubes in mice probed by Raman spectroscopy. *Proc. Natl Acad. Sci.* 105(5), 1410–1415 (2008).

40 Wall ME, Wani MC. Camptothecin and taxol: from discovery to clinic. *J. Ethnopharmacol.* 51(1), 239–254 (1996).

•• **Demonstrates paclitaxel loading onto single-walled nanotubes through covalent chemical bond to improve its solubility, biocompatibility and tumor targeting ability.**

41 Cavallaro G, Licciardi M, Caliceti P, Salmaso S, Giammona G. Synthesis, physico-chemical and biological characterization of a paclitaxel macromolecular prodrug. *Eur. J. Pharm. Biopharm.* V58(1), 151–159 (2004).

42 Allwood M, Martin H. The extraction of diethylhexylphthalate (DEHP) from polyvinyl chloride components of intravenous infusion containers and administration sets by paclitaxel injection. *Int. J. Pharm.* 127(1), 65–71 (1996).

43 Crosasso P, Ceruti M, Brusa P, Arpicco S, Dosio F, Cattel L. Preparation, characterization and properties of sterically stabilized paclitaxel-containing liposomes. *J. Control. Release* 63(1), 19–30 (2000).

44 Shuai X, Merdan T, Schaper AK, Xi F, Kissel T. Core-cross-linked polymeric micelles as paclitaxel carriers. *Bioconjug. Chem.* 15(3), 441–448 (2004).

45 Dong Y, Feng SS. *In vitro* and *in vivo* evaluation of methoxy polyethylene glycol–polylactide (MPEG–PLA) nanoparticles for small-molecule drug chemotherapy. *Biomaterials* 28(28), 4154–4160 (2007).

46 Skwarczynski M, Hayashi Y, Kiso Y. Paclitaxel prodrugs: toward smarter delivery of anticancer agents. *J. Med. Chem.* 49(25), 7253–7269 (2006).

47 Davis ME. Nanoparticle therapeutics: an emerging treatment modality for cancer. *Nat. Rev. Drug Discov.* 7(9), 771–782 (2008).

48 Lay CL, Liu HQ, Tan HR, Liu Y. Delivery of paclitaxel by physically loading onto poly(ethylene glycol) (PEG)-graft-carbon nanotubes for potent cancer therapeutics. *Nanotechnology* 21(6), 065101 (2010).

49 Xin J, Zhang R, Hou W. Assembly of gold nanoparticles on like-charge graphene oxide for fast release of hydrophobic molecules. *RSC Adv.* 4(12), 5834–5837 (2014).

50 Liu Z, Chen K, Davis C *et al.* Drug delivery with carbon nanotubes for *in vivo* cancer treatment. *Cancer Res.* 68(16), 6652–6660 (2008).

51 Deutsch H, Glinski J, Hernandez M *et al.* Synthesis of congeners and prodrugs. 3. Water-soluble prodrugs of taxol with potent antitumor activity. *J. Med. Chem.* 32(4), 788–792 (1989).

52 Dosio F, Brusa P, Crosasso P, Arpicco S, Cattel L. Preparation, characterization and properties in vitro and in vivo of a paclitaxel-albumin conjugate. *J. Control. Release* 47(3), 293–304 (1997).

53 Satoh T, Hosokawa M. The mammalian carboxylesterases: from molecules to functions. *Annu. Rev. Pharmacol. Toxicol.* 38(1), 257–288 (1998).

54 Liu Z, Cai W, He L *et al.* In vivo biodistribution and highly efficient tumour targeting of carbon nanotubes in mice. *Nat. Nanotechnol.* 2(1), 47–52 (2006).

55 Yang K, Gong H, Shi X, Wan J, Zhang Y, Liu Z. *In vivo* biodistribution and toxicology of functionalized nano-graphene oxide in mice after oral and intraperitoneal administration. *Biomaterials* 34(11), 2787–2795 (2013).

56 Zhang X, Yin J, Peng C *et al.* Distribution and biocompatibility studies of graphene oxide in mice after intravenous administration. *Carbon* 49(3), 986–995 (2011).

57 Hu W, Peng C, Lv M *et al.* Protein corona-mediated mitigation of cytotoxicity of graphene oxide. *ACS Nano* 5(5), 3693–3700 (2011).

58 Yang K, Li Y, Tan X, Peng R, Liu Z. Behavior and toxicity of graphene and its functionalized derivatives in biological systems. *Small* 9(9-10), 1492–1503 (2013).

59 Singh SK, Singh MK, Nayak MK *et al.* Thrombus inducing property of atomically thin graphene oxide sheets. *ACS Nano* 5(6), 4987–4996 (2011).

60 Singh SK, Singh MK, Kulkarni PP, Sonkar VK, Grácio JJ, Dash D. Amine-modified graphene: thrombo-protective safer alternative to graphene oxide for biomedical applications. *ACS Nano* 6(3), 2731–2740 (2012).

61 Liu Z, Fan AC, Rakhra K *et al.* Supramolecular stacking of doxorubicin on carbon nanotubes for *in vivo* cancer therapy. *Angew. Chem. Int. Ed.* 48(41), 7668–7672 (2009).

62 Liu Y, Wu DC, Zhang WD *et al.* Polyethylenimine-grafted multiwalled carbon nanotubes for secure noncovalent immobilization and efficient delivery of DNA. *Angew. Chem.* 117(30), 4860–4863 (2005).

63 Guengerich F, Peterson L, Böcker R. Cytochrome P-450-catalyzed hydroxylation and carboxylic acid ester cleavage of Hantzsch pyridine esters. *J. Biol. Chem.* 263(17), 8176–8183 (1988).

64 Morgan EW, Yan B, Greenway D, Petersen DR, Parkinson A. Purification and characterization of two rat-liver microsomal carboxylesterases (hydrolase A and B). *Archiv. Biochem. Biophys.* 315(2), 495–512 (1994).

65 Arya N, Arora A, Vasu KS, Sood AK, Katti DS. Combination of single walled carbon nanotubes/graphene oxide with paclitaxel: a reactive oxygen species mediated synergism for treatment of lung cancer. *Nanoscale* 5(7), 2818–2829 (2013).

66 Zhou L, Wang W, Tang J, Zhou JH, Jiang HJ, Shen J. Graphene oxide noncovalent photosensitizer and its anticancer activity *in vitro*. *Chemistry* 17(43), 12084–12091 (2011).